Published in final edited form as:
Ophthalmology. 2012 December ; 119(12): 2425–2433. doi:10.1016/j.ophtha.2012.06.023.

Corneal Epithelial Thickness Mapping by Fourier-domain Optical Coherence Tomography in Normal and Keratoconic Eyes

Yan Li, PhD[1], **Ou Tan, PhD**[1], **Robert Brass, MD**[2], **Jack L. Weiss, MD**[3], and **David Huang, MD, PhD**[1]

[1]Center for Ophthalmic Optics and Lasers (www.coollab.net), Casey Eye Institute and Department of Ophthalmology, Oregon Health and Science University, Portland, OR, USA 97239

[2]Brass Eye Center, Latham, NY, USA 12110

[3]Gordon & Weiss Vision Institute, San Diego, CA, USA 92122

Abstract

Objective—To map the corneal epithelial thickness with Fourier-domain optical coherence tomography (OCT) and develop epithelial thickness-based variables for keratoconus detection.

Design—Cross-sectional observational study.

Participants—One hundred forty-five eyes from 76 normal subjects and 35 keratoconic eyes from 22 patients.

Methods—A 26,000 Hz Fourier-domain OCT system with 5-μm axial resolution was used. The cornea was imaged with a “Pachymetry+Cpwr” scan pattern (6-mm scan diameter, 8 radials, 1024 axial-scans each, repeated 5 times) centered on the pupil. Three scans were obtained at a single visit in a prospective study. A computer algorithm was developed to automatically map the corneal epithelial thickness. Zonal epithelial thicknesses and 5 diagnostic variables, including minimum, superior–inferior (S-I), minimum–maximum (MIN-MAX), root-mean-square variation (RMSV), and root-mean-square pattern deviation (RMSPD), were calculated. Repeatability of the measurements was assessed by the pooled standard deviation. The area under the receiver operating characteristic curve (AROC) was used to evaluate diagnostic accuracy.

Main Outcome Measures—Descriptive statistics, repeatability, and AROC of the zonal epithelial thickness and diagnostic variables.

Results—The central, superior, and inferior epithelial thickness averages were 52.3±3.6, 49.6±3.5, and 51.2±3.4 μm in normal eyes and 51.9±5.3, 51.2±4.2 and 49.1±4.3 μm in keratoconic eyes. Compared to normal eyes, keratoconic eyes had significantly lower inferior (p =

Correspondence and reprint requests to: Yan Li, PhD, Casey Eye Institute, Oregon Health and Science University, 3375 SW Terwilliger Blvd, Portland, OR, USA 97239, liyan@ohsu.edu.

Partially presented at the American Society of Cataract and Refractive Surgery (ASCRS) annual meeting, April 2010, Boston, MA, USA, and the Association for Research in Vision and Ophthalmology (ARVO) annual meeting, May 2010, Fort Lauderdale, FL, USA.

Financial interest: Yan Li, Ou Tan, and David Huang have a significant financial interest in Optovue, Inc. (Fremont, CA, USA), a company that may have a commercial interest in the results of this research and technology. These potential conflicts of interest have been reviewed and managed by Oregon Health and Science University. Robert Brass receives speaker honoraria from Optovue, Inc. Jack L. Weiss has no proprietary interest in the topic of this manuscript.

0.03) and minimum corneal epithelial thickness ($p < 0.0001$), greater S-I ($p = 0.013$), more negative MIN-MAX ($p < 0.0001$), greater RMSV ($p < 0.0001$), and larger RMSPD ($p < 0.0001$). The repeatability of the zonal average, minimum, S-I, MIN-MAX epithelial thickness variables were between 0.7 to 1.9 μm. The repeatability of RMSV was better than 0.4 μm. The repeatability of RMSPD was 0.02 or better. Among all epithelial thickness based variables investigated, RMSPD provided the best diagnostic power (AROC = 1.00). Using a RMSPD cutoff value of 0.057 alone gave 100% specificity and 100% sensitivity.

Conclusions—High-resolution Fourier-domain OCT mapped corneal epithelial thickness with good repeatability in both normal and keratoconic eyes. Keratoconus was characterized by apical epithelial thinning. The resulting deviation from the normal epithelial pattern could be detected with very high accuracy using the RMSPD variable.

Keywords

Fourier-domain optical coherence tomography; corneal epithelial thickness map; keratoconus diagnosis

Introduction

The human corneal epithelium covers the surface of the cornea where it protects the eye and plays an important role in maintaining high optical quality. In diseases such as keratoconus, the thickness of the epithelium becomes altered to reduce corneal surface irregularity.[1] Therefore, the presence of an irregular stroma may be less measurable by frontal surface corneal topography. Analyzing the corneal epithelial and stromal thicknesses and shapes separately can facilitate the detection of the disease in its early stage.[1–3]

Several methods, such as confocal microscopy, ultrasound, and optical coherence tomography (OCT) have been used to measure corneal epithelial thickness. Many studies used these methods to measure the average central epithelium thickness.[4–7] Some used OCT to acquire peripheral epithelium thickness, but the number of points measured in the periphery was limited and the process was time consuming.[8] Very-high frequency ultrasound can map the corneal epithelium and stromal thickness over a wide area.[1, 9–11] However, this method is inconvenient as it requires immersion of the eye in a coupling fluid. Thus a non-contact method of epithelial mapping is still needed.

Optical coherence tomography is a non-contact technique that is based on the principles of low-coherence interferometry.[12] The high axial resolution allows excellent delineation of corneal surfaces. Time-domain anterior segment OCT systems can provide pachymetry (corneal thickness) maps.[13,14] Fourier-domain OCT, a newer generation of OCT, is capable of acquiring scans 10–100 times faster than time-domain OCT systems.[15–20] In this study, we developed software algorithms to automatically map corneal epithelial thickness in normal and keratoconic eyes imaged by a Fourier-domain OCT system. We also developed epithelial thickness-based diagnostic variables to facilitate keratoconus detection.

Methods

Subjects

Subjects of this cross-sectional observational study were recruited at Doheny Eye Institute at the University of Southern California (USC, Los Angeles, CA, USA), Brass Eye Center (Latham, NY, USA), Gordon & Weiss Vision Institute (San Diego, CA, USA), and Casey Eye Institute at Oregon Health and Science University (OHSU, Portland, OR, USA). This study followed the tenets of the Declaration of Helsinki and was in accord with the Health Insurance Portability and Accountability Act of 1996. The study protocol was approved by

the institutional review boards (IRBs) of USC, Oregon Health and Science University (Portland, OR, USA), and Western IRB (Olympia, WA, USA). Written informed consent was obtained from all subjects, all of whom were 18 or more years old.

Normal subjects were recruited from volunteers, patients seeking refractive surgery consultation, and patients seeking cataract surgery consultation. All had normal slit-lamp microscopy and normal topography. Normal subjects were divided into two groups for data analyzing purposes: Normal Group I and Normal Group II. The keratoconic eyes included in this study were diagnosed clinically. Each had corrected distance visual acuity (CDVA) equal or worse than 20/25 and had at least one clinical sign other than the keratoconic appearance of the topography map (asymmetric bow-tie with skewed radial axis, central or inferior steep zone, or claw-shape).[21–23] The kertatoconic slit-lamp findings included Munson's sign, Vogt's striae, Fleischer's ring, apical scar, apical thinning, or Rizutti's sign.[24] Eyes with late keratoconic changes such as corneal scars or hydrops were excluded as they have anomalous corneal epithelial findings and do not pose any diagnostic challenge. Contact lens wearers were not excluded from either group. None of the eyes had signs or history of other corneal disease, and none had undergone previous refractive or other ocular surgery.

Optical coherence tomography

A Fourier-domain OCT system (RTVue, Optovue Inc., Fremont, CA, USA) with a corneal adaptor module (CAM) was used in this study. The system worked at 830 nm wavelength and had a scan speed of 26,000 axial scans per second. The depth resolution was 5 μm (full-width-half-maximum) in tissue. The wide-angle (corneal long) adaptor lens used in this study provided a 6-mm long scan width with a transverse resolution of 15 μm (focused spot size).[17]

A "Pachymetry+Cpwr" scan pattern (6-mm scan diameter, 8 radials, 1024 axial-scans each, repeated 5 times) centered at the pupil center was used to map the cornea (Figure 1). RTVue-CAM software (software version 5.5) automatically processed the OCT scan to provide the pachymetry (corneal thickness) map and the minimum corneal thickness. Each eye was scanned 3 times within a single visit. Subjects were re-positioned after each OCT scan.

Fourier-domain OCT image data were exported and processed with custom software. For each OCT scan, 5 repeated radial cross-sectional images on each meridian were registered and averaged. Next the air-tear interface and the epithelium-Bowman's layer boundary were automatically identified with a computer algorithm by increased signal intensity at corresponding boundaries (Figure 2, available at http://aaojournal.org).[25] Then all boundaries detected were overlaid on the OCT image and verified by visual inspection (performed by YL). Unless otherwise specified, sets of scans were excluded from the following data analysis if the visual inspection identified boundary segmentation error on any meridional cross-sectional image. Eyes were excluded from data analysis if they had less than 2 scans with valid epithelium detection.

Corneal epithelial thickness was measured as the distance between the air-tear and the epithelium-Bowman's interfaces perpendicular to the anterior surface at the point of measurement. An epithelial thickness profile was generated from each meridional cross-section.

Topography

Corneal topography was obtained by either Orbscan II (Bausch & Lomb, Houston, TX, USA) or Pentacam (Oculus, Lynnwood, WA, USA) for all study subjects. The steep keratometry reading (steep K) of the simulated keratometry reading (SimK) was recorded.

Epithelial thickness maps and variables

A 6-mm diameter epithelial thickness map was generated by interpolating epithelial thickness profiles calculated from each meridian. Only the central 5-mm diameter map was used for calculating epithelial thickness-based variables.

Epithelial thickness map and zonal epithelial thicknesses—The epithelial thickness map was divided into 3 zones by diameter and hemispheres: central 2 mm, superior 2–5 mm, and inferior 2–5 mm (Figure 3A). The average epithelial thicknesses of central, superior, and inferior zones were calculated.

The average epithelial thickness maps of all normal subjects in Normal Group I were calculated for right and left eyes. The left eye maps were mirrored to the right eye to calculate the average map of both eyes. Similarly, the average epithelial thickness maps of all keratoconus subjects were calculated.

Epithelial thinning, focal thinning, and asymmetry—The minimum and maximum epithelial thicknesses were recorded, and the epithelial focal thinning was calculated as the difference between them (minimum-maximum, or MIN-MAX). Superior minus inferior asymmetry (superior-inferior, or S-I) was calculated by taking the difference between the average epithelial thicknesses of the superior and inferior zones.

Root-mean-square variation of the epithelial map—Root-mean-square variation (RMSV) from the average value of a single epithelial thickness map was calculated as

$$RMSV \text{ of the single epithelial map} = \sqrt{\frac{\sum_x \sum_y (\bar{T} - T(x,y))^2}{N}} \quad \text{Equation 1}$$

where $\bar{T}$ was the average epithelial thickness inside the 5-mm diameter area, and $T(x,y)$ was the epithelial thickness at map location (x, y). The origin (0, 0) was set to the map center. N was the total number of the map points inside the analytic zone ($\sqrt{x^2+y^2} \leq 2.5mm$).

Epithelial pattern deviation map—The epithelial pattern deviation map was calculated to show the difference between an individual epithelial pattern map and the average epithelial pattern map of normal subjects.

The epithelial pattern map of the normal reference population P_N was calculated as

$$P_N(x,y) = T_N(x,y) / \overline{T_N} \quad \text{Equation 2}$$

where T_N was the average epithelial thickness map of all normal subjects in Normal Group I, and $\overline{T_N}$ was the average thickness of map T_N.

Similarly, the individual epithelial pattern map P was calculated as

$$P(x,y)=T(x,y)/\overline{T} \quad \text{Equation 3}$$

where T was the individual epithelial thickness map, and $\bar{T}$ was the average thickness of the map.

The epithelial pattern deviation map (PD) was calculated as the difference between the individual epithelial pattern map (P) and the average normal epithelial pattern map (P_N):

$$PD(x,y)=P(x,y)-P_N(x,y) \quad \text{Equation 4}$$

Root-mean-square pattern deviation of the epithelial map—The root-mean-square pattern deviation (RMSPD) value was calculated from the pattern deviation map as

$$RMSPD=\sqrt{\frac{\sum_x\sum_y (PD(x,y))^2}{N}} \quad \text{Equation 5}$$

where $PD(x,y)$ was the epithelial pattern deviation value at map location (x,y). N was the total number of the map points inside the analytic zone.

Statistical analysis

Normal subjects older than 65-years-old were excluded from data analysis to match the age of keratoconus group. Descriptive statistics and other statistical analyses including *t*-tests were performed using MedCalc 12.0 software (MedCalc Software bvba, Mariakerke, Belgium). Mean ± standard deviation values of each corneal epithelial thickness variable were calculated for both normal and keratoconus groups. Repeatability of epithelial thickness variables were assessed by the pooled standard deviation obtained from the multiple measurements of each eye. The normality of OCT variables was confirmed by a Kolmogorov-Smirnov test on the dataset from which one eye was randomly selected from each normal subject.

To compare epithelial thickness variables measured in normal and keratoconic eyes, 2-tailed *t*-tests were performed. If both eyes of a subject were involved in the study, a randomly selected eye was chosen for the *t*-test to avoid the correlation between the two eyes from the same patient. P-values <0.05 were considered statistically significant.

Receiver operating characteristic (ROC) curve analyses were performed to evaluate the diagnostic performance of the epithelial thickness variables. Normal subjects in Normal Group II and all keratoconic subjects were involved in the ROC curve analyses. If both eyes of a subject were involved in the study, a randomly selected eye was chosen for the ROC curve analyses. The area under ROC curve (AROC) was calculated for each variable. A cutoff value of each variable was selected with the highest average of sensitivity and specificity. Corresponding sensitivity and specificity values were recorded. To assess the impact of segmentation errors on the diagnostic power of the epithelial thickness variables, separate ROC curve analyses were performed without excluding eyes and scans containing segmentation errors.

Results

Visual inspection confirmed that anterior corneal and epithelial boundary detection was satisfactory in 432 out of 435 normal scans (99.3%) and in 107 out of 114 keratoconic scans (93.9%). Three scans of normal eyes and 7 scans of keratoconic eyes were excluded from statistical analysis due to errors in boundary detection. Because the scans with segmentation errors occurred in different normal eyes, neither of those eyes was excluded. The keratoconic boundary detection errors resulted in the loss of 3 eyes from the study. In one example of a boundary detection error, the algorithm mistakenly identified the Bowman's-stroma interface instead of the epithelium-Bowman's interface (Figure 4A, available at http://aaojournal.org). A possible reason for this type of segmentation error was the increased reflectivity of the epithelium associated with a decrease in contrast at the central Bowman's layer and stroma. In a second example of a boundary detection error, a clear epithelium-Bowman's interface reflectivity peak was absent due to the fragmentation of Bowman's layer (Figure 4B, available at http://aaojournal.org).

Data were analyzed for 145 eyes of 76 normal subjects (29 men and 47 women) and 35 keratoconic eyes of 22 patients (12 men and 10 women). The average age of the normal subjects was 47.6 ± 13.9 years (range 19–65 years) and 43.9 ± 12.3 years (range 25–62 years) for keratoconus patients ($p = 0.25$). The steep K averaged 44.3 ± 1.5 diopter (D) (range 41.0 to 47.8 D) for all normal subjects and 48.6 ± 4.4 D (range 42.5–63.6 D) in the keratoconus group. The minimum corneal thickness was 530.4 ± 28.5 μm in normal eyes and 459.7 ± 50.5 μm in keratoconic eyes ($p < 0.0001$). The average base-10 logarithm of the minimum angle of resolution (LogMAR) CDVA was 0.21 in keratoconic eyes, equivalent to 20/32.3 Snellen acuity (range 20/25–20/200).

Fifty-four normal subjects were assigned to Normal Group I to calculate the normal reference population average epithelial thickness map (T_N) and the average normal epithelial pattern map (P_N). Twenty-two normal subjects were assigned to Normal Group II for ROC curve analyses. All 76 normal subjects were involved in all other statistical analyses.

The repeatability of epithelial thickness measurements in normal and keratoconic eyes were listed in Table 1. The repeatability of the zonal average, minimum, S-I, and minimum-maximum (MIN-MAX) epithelial thickness variables were between 0.7 and 1.9 μm. The repeatability of RMSV was better than 0.4 μm. The repeatability of RMSPD was 0.02 or better.

Significant differences in central and superior epithelial thickness values were not found between normal and keratoconic eyes ($p > 0.15$, Figure 3, Table 2). Compared to normal eyes, keratoconic eyes had a significantly thinner corneal epithelium inferiorly, lower minimum thickness, greater S-I, more negative MIN-MAX, greater RMSV, and larger RMSPD (Tables 2 and 3).

The typical epithelial thickness pattern deviation map of a normal eye showed small deviations (color green and uniform pattern) from the average normal pattern map (Figure 5A, available at http://aaojournal.org). In contrast, the pattern deviation map of a keratoconic eye contained large deviations (colors other than green and pattern uneven) from the average normal pattern map (Figure 5B, available at http://aaojournal.org). The average pattern deviation map of all keratoconic eyes (left eyes mirrored) showed that on average the epithelium was thinner inferotemporally and thicker superonasally in keratoconic eyes than in normal eyes (Figure 6).

For the variables minimum, MIN-MAX, and RMSV, there was considerable overlap between the normal and keratoconic eyes (Figure 7). The least overlap occurred with RMSPD. Using the RMSPD cutoff value of 0.057 alone gave 100% specificity and 100% sensitivity (Table 4).

For ROC analyses excluding eyes and scans containing segmentation errors, RMSPD provided the best diagnostic power (AROC = 1.0, Table 4) among all of the epithelial thickness-based variables investigated in this study. The diagnostic power of other variables (Table 4) varied from poor (central, superior, and inferior zonal epithelial thicknesses), to fair (S-I), to good (minimum, MIN-MAX and RMSV). Even for ROC analyses including eyes and scans containing segmentation errors, the AROC of RMSPD was 1.00, and the AROCs of the other diagnostic variables changed less than 0.01.

One normal, one mild keratoconus, and one advanced keratoconus cases were shown in Figure 8 (available at http://aaojournal.org).

Discussion

Fourier-domain OCT instruments can provide scan speeds 10–100 times faster than time-domain OCT instruments.[26] The enhanced speeds minimize the effect of eye movements during data acquisition, and also allow higher definition imaging due to denser axial scans in the same transverse scan length. The higher scan speed also facilitates frame averaging that suppresses speckle noise. The epithelium-Bowman's layer boundary is a relatively weak interface presented in corneal OCT images. In this study, we enhanced the epithelial boundary by acquiring 5 repeated images and averaging them after the registration. The averaged image had higher signal-to-noise ratio than the single frame. Moreover, the Fourier-domain OCT system used in our study had an axial resolution of 5 μm, which is 2–3 times higher than that of time-domain instruments used in previous studies.[6, 27–29] Not only does the higher resolution and higher speed of Fourier-domain OCT improve image quality, it also makes the automated corneal epithelial thickness mapping possible.

The corneal epithelium is the first cellular layer of the human cornea and protects the eye. Accurate and reproducible measurement of corneal epithelial thickness provides important information for assessing corneal remodeling after refractive surgeries such as photorefractive keratectomy and LASIK.[30] Moreover, deviations from normal epithelial thickness could be an early sign of keratoconus.[1] Many efforts had been made to measure the corneal epithelial thickness (Table 5). Li,[4] Erie,[5] Patel[31] and their colleagues reported central epithelial thicknesses of 41–50.6 μm in normal corneas measured by confocal microscopy. Their measurements, which excluded the pre-corneal tear film thickness, were thinner than the central epithelial thickness of 52.3 ± 3.6 μm in normal eyes that we obtained. Our measurements included the thickness of tear film, about 3 μm,[32] which probably accounts for the difference. Reinstein et al. pioneered corneal epithelial thickness mapping using very high frequency ultrasound over the entire corneal surface.[1, 9, 10] The central epithelial thickness of normal eyes from their study, which excluded the tear film, was 53.4 ± 4.6 μm.[9] Their research also demonstrated that corneal epithelium was thicker inferiorly than superiorly in the normal corneas.[9] Our observation (S-I mean difference = −1.6 μm) agreed with their results.

Optical coherence tomography is a non-contact imaging method with high axial resolution. Several investigators used time-domain OCT systems to measure corneal epithelial thickness. Among them, Sin,[6] Haque,[28] Feng[29] and their colleagues reported central corneal epithelial thicknesses of 52–54.7 μm in normal eyes, values that are very close to our measurements. In contrast, Wang et al., also using a time-domain system, reported a thicker

value, 59.9 ± 5.9 μm.[27] Recently, Tao el al. used a custom-built Fourier-domain OCT to measure central epithelial thickness in normal subjects.[33] Their finding of 52.5 ± 2.4 μm was similar to our own. Francoz et al. used a commercial Fourier-domain OCT to measure central epithelial thickness in young adults (< 40 years) and middle-age adults (>40 years) and found that the thickness was similar, ~48.5 μm, for the two groups.[34] They excluded the pre-corneal tear film from the thickness determinations, which probably explains why their values were thinner than the ones we measured.

Keratoconus is a degenerative condition in which the cornea progressively displays an irregular, cone-like shape. It is an important contraindication for refractive surgeries such as LASIK and photorefractive keratectomy. Undetected keratoconus can result in accelerated, progressive keratoectasia and unpredictable outcomes after the surgery.[35–40] Haque et al. reported that the central epithelial thickness in individuals with keratoconus was 4.7 μm thinner than the control thickness.[28] Reinstein et al. found that the central epithelial thickness in keratoconic eyes, 45.7 ± 5.9 μm, was significantly thinner than in normal eyes.[1] In our study, statistically significant difference was not detected. One possibility was that the ectasia was usually located inferotemporally in the keratoconic corneas. The ultrasound scan in the Reinstein's study was centered on corneal vertex which was shifted inferotemporally in keratoconus. The OCT scan in our study was centered on the pupil, which was not displaced by the cone location. On the other hand, we did find that the minimum corneal epithelial thickness in keratoconic eyes, 40.0 ± 6.0 μm, was significantly thinner than normal eyes, 46.0 ± 4.3 μm. In addition to their interesting finding that epithelial thinning occurred at the apex of the cone, Reinstein et al. also showed that the zone of epithelial thinning was surrounded by an annulus of thicker epithelium.

Previously we developed a mathematical model to describe epithelial smoothing in response to corneal contour change after laser refractive surgery.[30] Reinstein et al. indicated that the epithelium appears to remodel to eliminate or reduce the bulging of the anterior stromal surface.[1] Both suggest that epithelial smoothing may play an important role in reducing the irregularity of the anterior stromal surface in keratoconus. Moreover, we observed greater S-I and MIN-MAX epithelial thickness differences, greater RMSVs, and larger RMSPDs. All demonstrated that corneal epithelial thickness variation was significantly increased in keratoconic eyes.

Several corneal epithelial thickness-based variables developed in this study showed good (minimum, AROC = 0.84; MIN-MAX, AROC = 0.88; RMSV, AROC = 0.89) to excellent (RMSPD, AROC = 1.00) diagnostic power in differentiating keratoconic from normal eyes. By far, RMSPD was the best variable. With a cutoff value of 0.057, RMSPD alone gave 100% specificity and 100% sensitivity. These variables could be applied to epithelial thickness maps from other imaging systems as well (for example, very-high frequency ultrasound). Moreover, these variables may be useful for detecting *forme fruste* keratoconus (FFK, or sub-clinical keratoconus). Further studies are needed to evaluate the performance of these variables in FFK detection.

One limitation of the technology used in this study is that RTVue-CAM OCT provides pachymetric and epithelial thickness maps of only the central 6-mm diameter of the cornea. The 6-mm map size may be sufficient for planning myopic LASIK and photorefractive keratectomy since the central corneal tissue is ablated most for myopic refractive surgery procedures. It may be sufficient for keratoconus screening because a previous study showed that the cone apex was located inside the central 5-mm diameter of the cornea in the vast majority of keratoconic eyes.[41] However, the 6-mm map size is a limitation for diseases involving the peripheral cornea, such as pellucid marginal degeneration. Moreover, we did not observe a full ring of thicker epithelium surrounding the localized corneal thinning as

presented by Reinstein et al. A larger epithelial map size may facilitate further comparison on epithelial thickness map patterns.

Another limitation of the technology is segmentation error by the automated epithelial boundary detection algorithm in a small percentage of scans. These failures tend to occur in keratoconic eyes. The errors were associated with higher central epithelial reflectivity or reduced contrast between the Bowman's layer and stroma. The higher epithelial reflectivity could be caused by chronic rubbing from rigid gas permeable (RGP) contact lens wear. The loss of a distinct reflectivity peak in Bowman's layer in some keratoconic eyes could be explained by thinning or fragmentation of Bowman's layer, which occurs in this disease. Since low contrast between the epithelium, Bowman's layer, and anterior stroma are associated with these segmentation errors, an automated grading system could be developed based on the contrast to warn users when the reliability of the epithelial thickness measurement is low. Nevertheless, ROC analyses showed that segmentation error did not affect the discrimination between normal and keratoconic eyes in this study. One reason is that the segmentation error was small, no more than the thickness of the Bowman's layer.[33] Also, the segmentation error typically occurred only in a small part of the eight cross-sectional meridional scans. Thus for the purpose keratoconus detection, these small segmentation errors do not present a practical problem. However, the reliability of epithelial thickness mapping in other situations where the contrast between the epithelium and subjacent layers are altered, such as post-phototherapeutic keratectomy eyes, requires further study before this method can be confidently applied.

RGP contact lenses wearing could produce apical epithelial thinning. This thinning effect may be combined with the epithelial thinning due to keratoconus in keratoconic subjects who wearing RGP contact lens. It's a limitation of the present study that we did not collect contact lens history and record the time between contact lens removal and examination. This deserves more attention in future studies. Nevertheless, the best diagnostic variable of this study - RMSPD - had 100% specificity and sensitivity with mixed subjects of contact lens users and non-users. The specificity and sensitivity would have remained 100% if the ROC analysis had been performed separating the contact lens users and non-users.

In summary, we used high-resolution Fourier-domain OCT to successfully map corneal epithelial thickness with good repeatability in both normal and keratoconic eyes. Keratoconus was characterized by apical epithelial thinning. The resulting deviation from the normal epithelial pattern could be detected with very high accuracy using the RMSPD variable.

Supplementary Material

Refer to Web version on PubMed Central for supplementary material.

Acknowledgments

The authors would like to thank Dr. Qienyuan Zhou for coordinating study data collection, Dr. Xinbo Zhang for consultation in statistics, and Dr. Maolong Tang for consultation on corneal topography.

Financial Support: NIH grant R01EY018184, a research grant from Optovue, Inc., and an unrestricted grant to Casey Eye Institute from Research to Prevent Blindness

References

1. Reinstein DZ, Gobbe M, Archer TJ, et al. Epithelial, stromal, and total corneal thickness in keratoconus: three-dimensional display with Artemis very-high frequency digital ultrasound. J Refract Surg. 2010; 26:259–71. [PubMed: 20415322]

2. Reinstein DZ, Archer TJ, Gobbe M. Corneal epithelial thickness profile in the diagnosis of keratoconus. J Refract Surg. 2009; 25:604–10. [PubMed: 19662917]
3. Reinstein DZ, Archer TJ, Gobbe M. Stability of LASIK in topographically suspect keratoconus confirmed non-keratoconic by Artemis VHF digital ultrasound epithelial thickness mapping: 1-year follow-up. J Refract Surg. 2009; 25:569–77. [PubMed: 19662913]
4. Li HF, Petroll WM, Moller-Pedersen T, et al. Epithelial and corneal thickness measurements by in vivo confocal microscopy through focusing (CMTF). Curr Eye Res. 1997; 16:214–21. [PubMed: 9088737]
5. Erie JC, Patel SV, McLaren JW, et al. Effect of myopic laser in situ keratomileusis on epithelial and stromal thickness: a confocal microscopy study. Ophthalmology. 2002; 109:1447–52. [PubMed: 12153794]
6. Sin S, Simpson TL. The repeatability of corneal and corneal epithelial thickness measurements using optical coherence tomography. Optom Vis Sci. 2006; 83:360–5. [PubMed: 16772894]
7. Wang J, Fonn D, Simpson TL, Jones L. The measurement of corneal epithelial thickness in response to hypoxia using optical coherence tomography. Am J Ophthalmol. 2002; 133:315–9. [PubMed: 11860966]
8. Haque S, Jones L, Simpson T. Thickness mapping of the cornea and epithelium using optical coherence tomography. Optom Vis Sci. 2008; 85:E963–76. [PubMed: 18832971]
9. Reinstein DZ, Archer TJ, Gobbe M, et al. Epithelial thickness in the normal cornea: three-dimensional display with Artemis very high-frequency digital ultrasound. J Refract Surg. 2008; 24:571–81. [PubMed: 18581782]
10. Reinstein DZ, Archer TJ, Gobbe M, et al. Epithelial thickness after hyperopic LASIK: three-dimensional display with Artemis very high-frequency digital ultrasound. J Refract Surg. 2010; 26:555–64. [PubMed: 19928697]
11. Reinstein DZ, Silverman RH, Raevsky T, et al. Arc-scanning very high-frequency digital ultrasound for 3D pachymetric mapping of the corneal epithelium and stroma in laser in situ keratomileusis. J Refract Surg. 2000; 16:414–30. [PubMed: 10939721]
12. Huang D, Swanson EA, Lin CP, et al. Optical coherence tomography. Science. 1991; 254:1178–81. [PubMed: 1957169]
13. Li Y, Shekhar R, Huang D. Corneal pachymetry mapping with high-speed optical coherence tomography. Ophthalmology. 2006; 113:792–9. [PubMed: 16650675]
14. Li EY, Mohamed S, Leung CK, et al. Agreement among 3 methods to measure corneal thickness: ultrasound pachymetry, Orbscan II, and Visante anterior segment optical coherence tomography. Ophthalmology. 2007; 114:1842–7. [PubMed: 17507097]
15. Christopoulos V, Kagemann L, Wollstein G, et al. In vivo corneal high-speed, ultra high-resolution optical coherence tomography. Arch Ophthalmol. 2007; 125:1027–35. [PubMed: 17698748]
16. Ko TH, Fujimoto JG, Duker JS, et al. Comparison of ultrahigh- and standard-resolution optical coherence tomography for imaging macular hole pathology and repair. Ophthalmology. 2004; 111:2033–43. [PubMed: 15522369]
17. Li Y, Tang ML, Zhang XB, et al. Pachymetric mapping with Fourier-domain optical coherence tomography. J Cataract Refract Surg. 2010; 36:826–31. [PubMed: 20457376]
18. Sarunic MV, Asrani S, Izatt JA. Imaging the ocular anterior segment with real-time, full-range Fourier-domain optical coherence tomography. Arch Ophthalmol. 2008; 126:537–42. [PubMed: 18413525]
19. Wojtkowski M, Leitgeb R, Kowalczyk A, et al. In vivo human retinal imaging by Fourier domain optical coherence tomography. J Biomed Opt. 2002; 7:457–63. [PubMed: 12175297]
20. Yasuno Y, Madjarova VD, Makita S, et al. Three-dimensional and high-speed swept-source optical coherence tomography for in vivo investigation of human anterior eye segments. Opt Express [serial online]. 2005; 13:10652–64. Available at: http://www.opticsinfobase.org/oe/abstract.cfm?uri=oe-13-26-10652.
21. Binder PS, Lindstrom RL, Stulting RD, et al. Keratoconus and corneal ectasia after LASIK. J Refract Surg. 2005; 21:749–52. [PubMed: 16329368]
22. Jafri B, Li X, Yang H, Rabinowitz YS. Higher order wavefront aberrations and topography in early and suspected keratoconus. J Refract Surg. 2007; 23:774–81. [PubMed: 17985796]

23. Lee BW, Jurkunas UV, Harissi-Dagher M, et al. Ectatic disorders associated with a claw-shaped pattern on corneal topography. Am J Ophthalmol. 2007; 144:154–6. [PubMed: 17601448]
24. Rabinowitz YS. Keratoconus. Surv Ophthalmol. 1998; 42:297–319. [PubMed: 9493273]
25. Li, Y.; Tan, O.; Huang, D. Normal and keratoconic corneal epithelial thickness mapping using Fourier-domain optical coherence tomography. In: Weaver, JB.; Molthen, RC., editors. Medical Imaging 2011: Biomedical Applications in Molecular, Structural, and Functional Imaging. Bellingham, WA: SPIE; 2010. p. 796508
26. Fujimoto, J.; Huang, D. Introduction to optical coherence tomography. In: Huang, D.; Duker, J.; Fujimoto, J., et al., editors. Imaging the Eye from Front to Back with RTVue Fourier-Domain Optical Coherence Tomography. Thorofare, NJ: SLACK; 2010. p. 1-21.
27. Wang J, Thomas J, Cox I, Rollins A. Noncontact measurements of central corneal epithelial and flap thickness after laser in situ keratomileusis. Invest Ophthalmol Vis Sci. 2004; 45:1812–6. [PubMed: 15161844]
28. Haque S, Simpson T, Jones L. Corneal and epithelial thickness in keratoconus: a comparison of ultrasonic pachymetry, Orbscan II, and optical coherence tomography. J Refract Surg. 2006; 22:486–93. [PubMed: 16722488]
29. Feng Y, Simpson TL. Corneal, limbal, and conjunctival epithelial thickness from optical coherence tomography. Optom Vis Sci. 2008; 85:E880–3. [PubMed: 18772715]
30. Huang D, Tang M, Shekhar R. Mathematical model of corneal surface smoothing after laser refractive surgery. Am J Ophthalmol. 2003; 135:267–78. [PubMed: 12614741]
31. Patel SV, Erie JC, McLaren JW, Bourne WM. Confocal microscopy changes in epithelial and stromal thickness up to 7 years after LASIK and photorefractive keratectomy for myopia. J Refract Surg. 2007; 23:385–92. [PubMed: 17455834]
32. Azartash K, Kwan J, Paugh JR, et al. Pre-corneal tear film thickness in humans measured with a novel technique. Mol Vis [serial online]. 2011; 17:756–67. Available at: http://www.molvis.org/molvis/v17/a86/.
33. Tao A, Wang J, Chen Q, et al. Topographic thickness of Bowman's layer determined by ultra-high resolution spectral domain-optical coherence tomography. Invest Ophthalmol Vis Sci. 2011; 52:3901–7. [PubMed: 21460260]
34. Francoz M, Karamoko I, Baudouin C, Labbe A. Ocular surface epithelial thickness evaluation with spectral-domain optical coherence tomography. Invest Ophthalmol Vis Sci. 2011; 52:9116–23. [PubMed: 22025572]
35. Amoils SP, Deist MB, Gous P, Amoils PM. Iatrogenic keratectasia after laser in situ keratomileusis for less than −4.0 to −7. 0 diopters of myopia. J Cataract Refract Surg. 2000; 26:967–77. [PubMed: 10946186]
36. Binder PS, Lindstrom RL, Stulting RD, et al. Keratoconus and corneal ectasia after LASIK [letter]. J Cataract Refract Surg. 2005; 31:2035–8. [PubMed: 16412891]
37. Krachmer JH, Feder RS, Belin MW. Keratoconus and related noninflammatory corneal thinning disorders. Surv Ophthalmol. 1984; 28:293–322. [PubMed: 6230745]
38. Randleman JB, Russell B, Ward MA, et al. Risk factors and prognosis for corneal ectasia after LASIK. Ophthalmology. 2003; 110:267–75. [PubMed: 12578766]
39. Seiler T, Quurke AW. Iatrogenic keratectasia after LASIK in a case of forme fruste keratoconus. J Cataract Refract Surg. 1998; 24:1007–9. [PubMed: 9682124]
40. Randleman JB, Woodward M, Lynn MJ, Stulting RD. Risk assessment for ectasia after corneal refractive surgery. Ophthalmology. 2008; 115:37–50. [PubMed: 17624434]
41. Tang M, Shekhar R, Miranda D, Huang D. Characteristics of keratoconus and pellucid marginal degeneration in mean curvature maps. Am J Ophthalmol. 2005; 140:993–1001. [PubMed: 16376641]
42. Ladage PM, Yamamoto K, Ren DH, et al. Effects of rigid and soft contact lens daily wear on corneal epithelium, tear lactate dehydrogenase, and bacterial binding to exfoliated epithelial cells. Ophthalmology. 2001; 108:1279–88. [PubMed: 11425688]

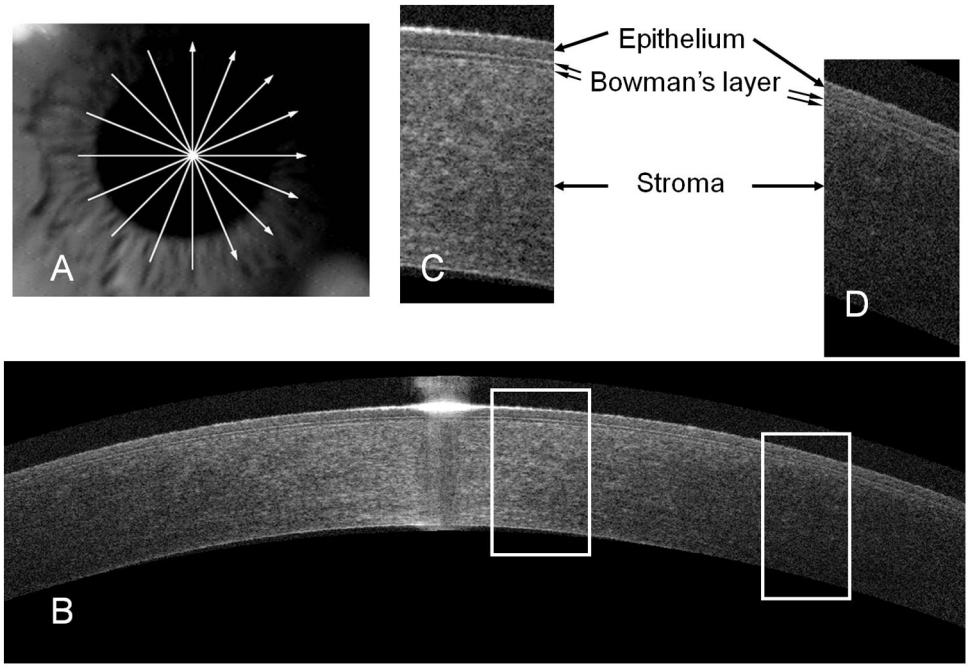

Figure 1.
A: "Pachymetry+Cpwr" scan pattern consisted of 8 radial scans. B: A cross-sectional corneal optical coherence tomography (OCT) image (average of 5 repeated frames). C and D: Magnified sections of the OCT image shown in B.

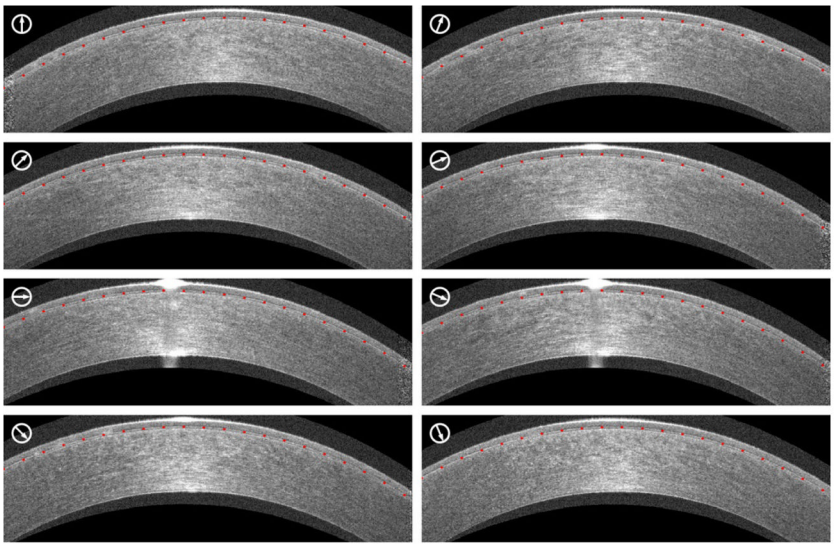

Figure 2.
Corneal epithelial boundaries (delineated by red dots) were identified in all eight meridians.

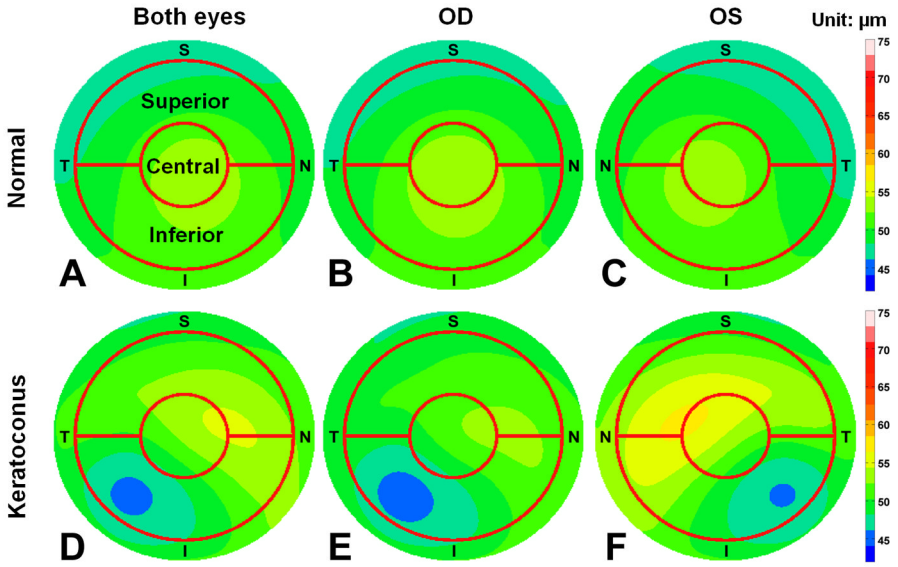

Figure 3.
Average epithelial thickness maps of normal (A–C) and keratoconic eyes (D–F). Left column (A, D): All eyes were included with left eyes mirrored. Middle column (B, E): Right eyes (OD) only. Right column (C, F): Left eyes (OS) only. S = superior, I = inferior, T = temporal, N = nasal. The red circles overlaid on the map had diameters of 2 and 5 mm. The color scale represents the thickness in micrometers.

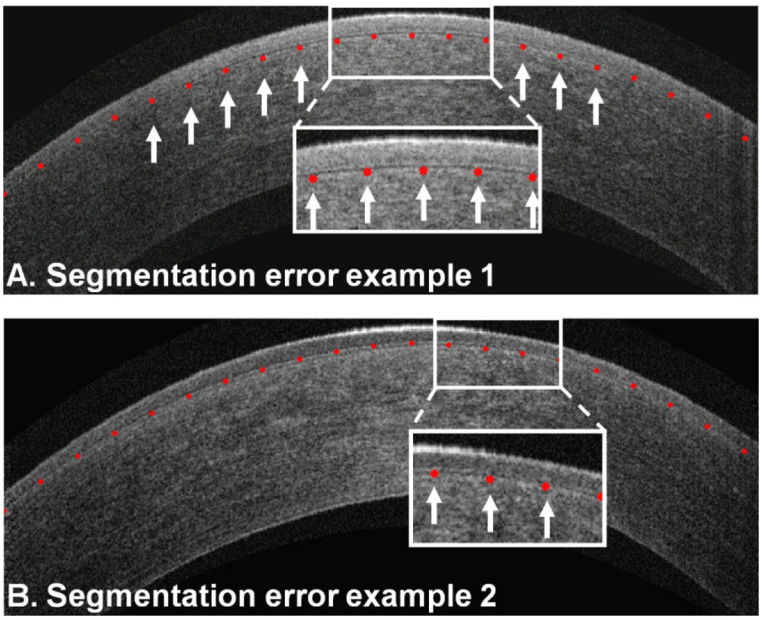

Figure 4.
Examples of typical epithelium segmentation errors. The algorithm mistakenly identified Bowman's-stroma interface instead of epithelium-Bowman's interface at locations marked by arrows. (Insets) Magnified sections of the optical coherence tomography images.

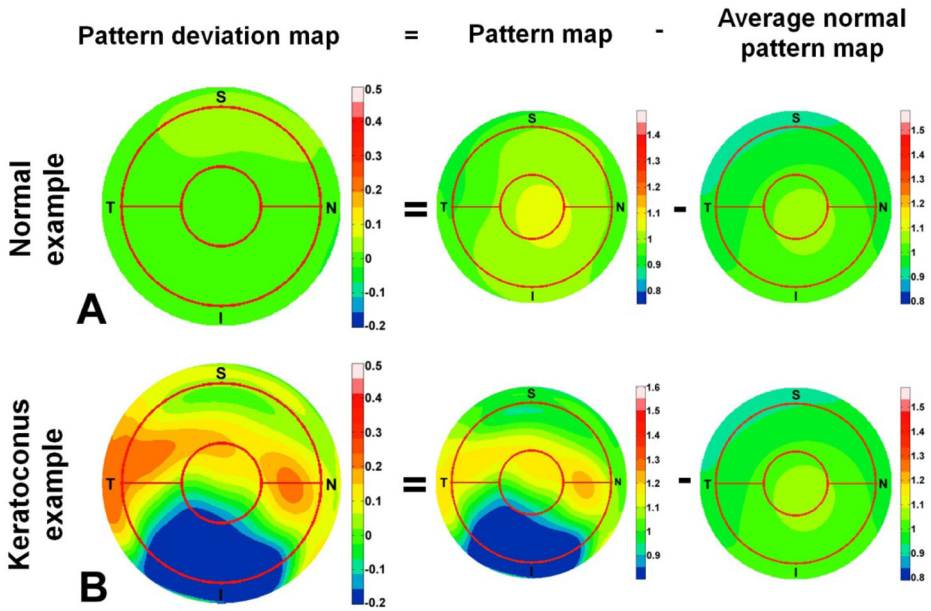

Figure 5.

The corneal epithelial thickness pattern deviation map (left) was calculated by subtracting the average normal pattern map (right) from the individual pattern map (middle). A: a normal example. B: a keratoconus example. S = superior, I = inferior, T = temporal, N = nasal. The color scale represents pattern deviation with no units.

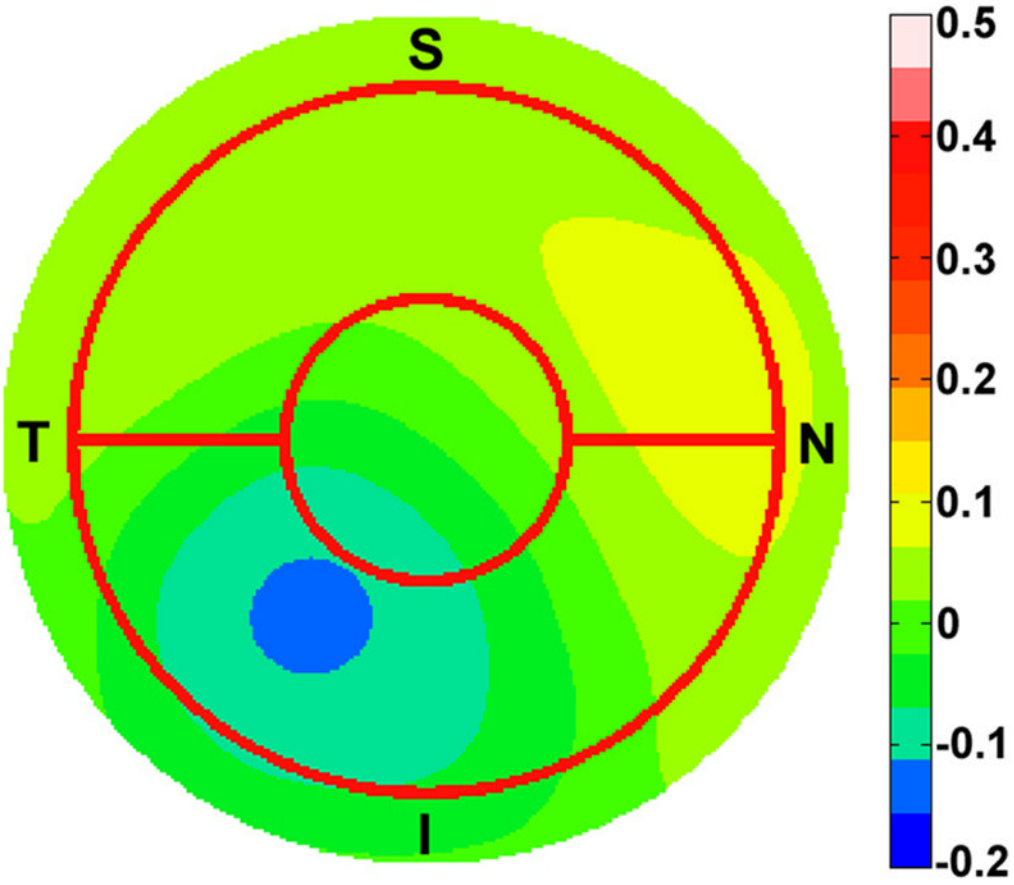

Figure 6.
Average corneal epithelial thickness pattern deviation map of keratoconic eyes. All eyes were included with left eyes mirrored. S = superior, I = inferior, T = temporal, N = nasal. The color scale represents pattern deviation with no units.

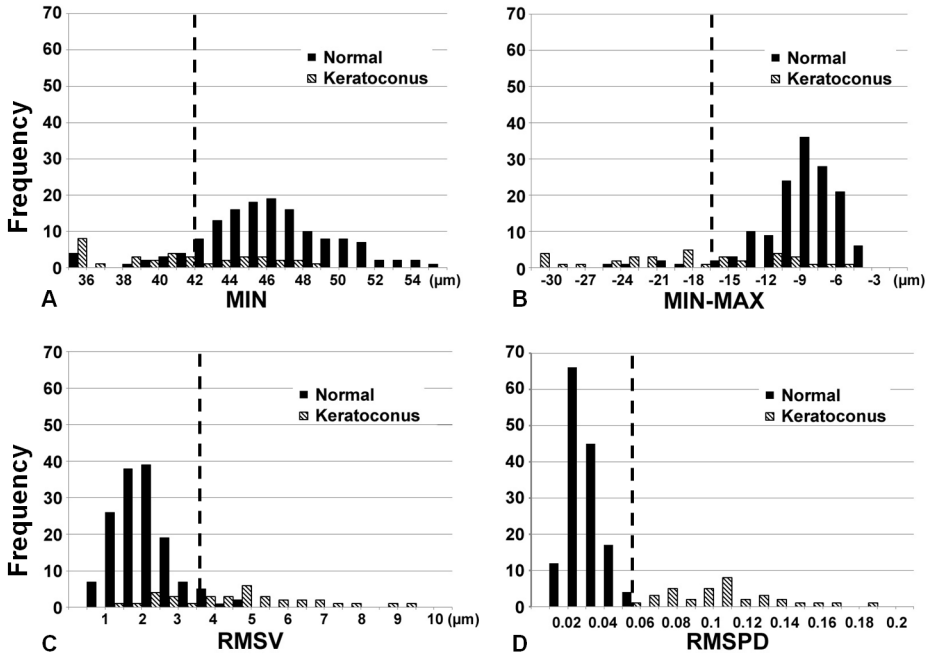

Figure 7.
Histograms of 4 corneal epithelial thickness-based variables. A: Minimum (MIN). B: Minimum-maximum (MIN-MAX). C: Root-mean-square variation (RMSV). D. Root-mean-square pattern deviation (RMSPD). Dashed lines indicated optimized cut-off values of the variables.

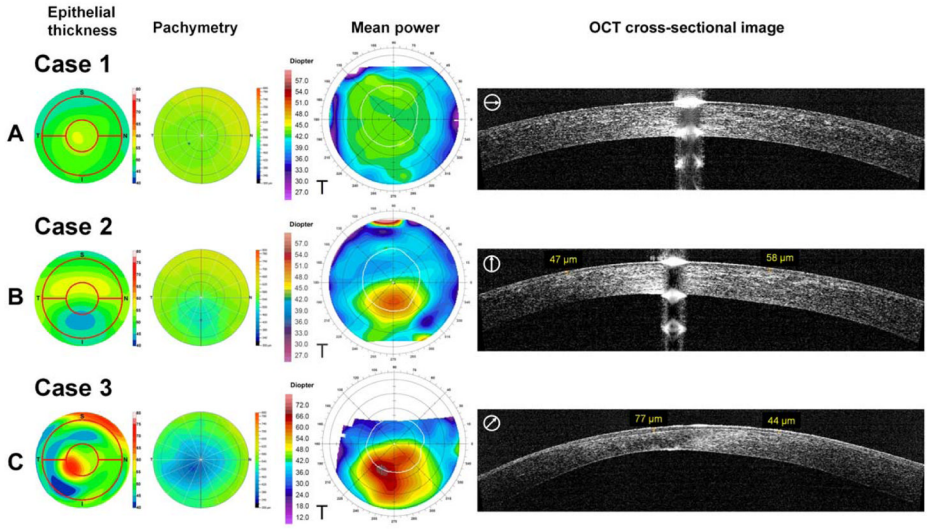

Figure 8.

Corneal epithelial thickness, pachymetric, topographic mean power maps, and cross-sectional optical coherence tomography (OCT) images of three cases. S = superior, I = inferior, T = temporal, N = nasal.

Case 1 (A) was a randomly chosen normal right eye of a 37-year-old man. The corrected distance visual acuity (CDVA) was 20/20. The topographic simulated keratometry (SimK) readings were 42.2 diopter (D) and 43.0 D. The epithelial thickness was relatively uniform. Case 2 (B) was a 29-year-old woman with mild keratoconus in her right eye. The CDVA was 20/25. The SimKs were 42.9 and 44.7 D. The epithelial thickness map showed inferior epithelial thinning and relatively large epithelial thickness variation with superior-inferior (S-I) = 6.7 μm, root-mean-square variation (RMSV) = 4.3 μm, and root-mean-square pattern deviation (RMSPD) = 0.064. The pachymetry map showed inferior corneal thinning. The topographic mean power map revealed that the cone apex was located approximately 1.5 mm inferior to the pupil center. The epithelial thinning and the corneal thinning were both located over the cone. Case 3 (C) was a 33-year-old man with advanced keratoconus in his right eye. The CDVA was 20/200. The SimKs were 56.1 and 63.6 D. The epithelial thickness map showed thinning approximately 2 mm from the pupil center, and thickening about 1 mm from the pupil center, both inferotemporally. The epithelial thickness variation was large with the minimum = 38.1 μm, S-I = 0.07 μm, minimum-maximum (MIN-MAX) = −32.1 μm, RMSV = 6.1 μm, and RMSPD = 0.112. The pachymetry map showed inferotemporal corneal thinning. The cone apex was 2 mm inferotemporal to the pupil center. The thinnest epithelium was located over the cone apex as defined by point of greatest mean power. The epithelium was actually thicker than the average at the thinnest location of the cornea.

Table 1

Repeatability of corneal epithelial thickness parameters by pooled-standard deviation

	N	Central	Superior	Inferior	MIN	S-I	MIN-MAX	RMSV	RMSPD†
Normal	145	0.7	0.8	0.7	1.1	0.7	1.1	0.2	0.008
Keratoconus	35	1.0	1.0	1.0	1.8	1.3	1.9	0.4	0.020

N = number of eyes; S-I = superior-inferior; MIN = minimum; MIN-MAX = minimum-maximum; RMSV = root-mean-square variation; RMSPD = root-mean-square pattern deviation

† RMSPD was without units; all other variables had units of μm.

Table 2

Epithelial map zonal thickness variables

	N	Central	Superior	Inferior	MIN
Normal	145	52.3 ± 3.6	49.6 ± 3.5	51.2 ± 3.4	46.0 ± 4.3
Keratoconus	35	51.9 ± 5.3	51.2 ± 4.2	49.1 ± 4.3	40.0±6.0
T-test p-value *		0.42	0.15	0.03	<0.0001

MIN = minimum.

Descriptive statistics had units of μm.

* The fellow eye was excluded from *t*-tests to eliminate the correlation between the two eyes of a subject.

Table 3

Epithelial map uniformity indices

	N	S-I	MIN-MAX	RMSV	RMSPD†
Normal	145	−1.6 ± 1.8	−8.8 ± 3.5	2.1 ± 0.8	0.030±0.009
Keratoconus	35	2.1 ± 5.4	−18.7±8.0	4.7 ± 2.0	0.105±0.030
T-test p-value *		0.013	< 0.0001	< 0.0001	< 0.0001

MIN-MAX = minimum-maximum; RMSV = root-mean-square variation; RMSPD = root-mean-square pattern deviation

† RMSPD was without units; descriptive statistics of all other variables had units of μm.

* The fellow eye was excluded from *t*-tests to eliminate the correlation between the two eyes of a subject.

Table 4

Cut off criterion, sensitivity, specificity, and area under the receiver operating characteristic curve of epithelial thickness variables.

	Central	Superior	Inferior	MIN	S-I	MIN-MAX	RMSV	RMSPD†
Criterion	<48.4	>51.9	<48.1	<41.8	>0.0	<−16.3	>3.6	>0.057
Sensitivity	31.8	50.0	31.8	63.6	68.2	68.2	72.7	100
Specificity	100	72.7	95.5	95.5	81.8	95.5	95.5	100
AROC	0.61	0.57	0.64	0.84	0.73	0.88	0.89	1.00
95% CI	0.45 to 0.75	0.41 to 0.72	0.48 to 0.78	0.69 to 0.93	0.58 to 0.86	0.75 to 0.96	0.76 to 0.97	0.92 to 1.0

MIN = minimum; S-I = superior-inferior; MIN-MAX = minimum-maximum; RMSV = root-mean-square variation; RMSPD = root-mean-square pattern deviation; AROC = area under the receiver operating characteristic curve; CI = confidence interval

†RMSPD was without units; criteria of all other variables had units of μm

Table 5

Central corneal epithelial thickness reported by previous investigators

	Normal (μm)	Keratoconus (μm)	Instrument used
Li et al.[4]	50.6 ± 3.9 *		Confocal microscopy
Erie et al.[5]	46 ± 5 *		Confocal microscopy
Patel et al.[31]	41 ± 4 *		Confocal microscopy
Reinstein et al.[1, 9]	53.4 ± 4.6 *	45.7 ± 5.9 *	Very-high frequency ultrasound
Wang et al.[27]	59.9 ± 5.9		Time-domain OCT
Sin et al.[6]	52 ± 3		Time-domain OCT
Haque et al.[28]	52.9 ± 4.1	48.2 ± 5.5	Time-domain OCT
Feng et al.[29]	54.7 ± 1.9		Time-domain OCT
Tao et al.[33]	52.5 ± 2.4		Fourier-domain OCT
Francoz et al.[34]	48.3 ± 2.9 *		Fourier-domain OCT
This study	52.3 ± 3.6	51.9 ± 5.3	Fourier-domain OCT

OCT = optical coherence tomography

* Pre-corneal tear thickness was excluded